Diagnostic and Interventional Imaging (2015) 96, 1177—1188

ORIGINAL ARTICLE /*Musculoskeletal imaging*

Radiography of scoliosis: Comparative dose levels and image quality between a dynamic flat-panel detector and a slot-scanning device (EOS system)

M. Yvert[a], A. Diallo[b], P. Bessou[a], J.-L. Rehel[c], E. Lhomme[b], J.-F. Chateil[a,d,*]

[a] *Service d'imagerie anté-natale, de l'enfant et de la femme, Hôpital Pellegrin, place Amélie-Raba-Léon, 33076 Bordeaux cedex, France*
[b] *Institute of Public Health, Epidemiology and Development (ISPED), Université de Bordeaux, 146, rue Léo-Saignat, 33076 Bordeaux cedex, France*
[c] *Institute for Radiological Protection and Nuclear Safety (IRSN), 31, avenue de la Division-Leclerc, 92260 Fontenay-aux-Roses, France*
[d] *Centre de Résonance Magnétique des Systèmes Biologiques, UMR 5536, Université de Bordeaux, 146, rue Léo-Saignat, 33076 Bordeaux cedex, France*

KEYWORDS
Children;
Scoliosis;
Image quality enhancement;
Radiation dose;
Radiation protection

Abstract
Purpose: To compare radiation dose and image quality between a slot-scanning system (SSS) and a dynamic flat-panel detector (DFD) in assessing scoliosis in children.
Methods: An experimental study was first performed with a phantom to assess the quality of each device. The clinical part included a prospective observational dosimetric and qualitative comparative study with acquisition of whole-spine X-ray: SSS (31 children), DFD (26 children). Institutional review board approval and informed consent were obtained. Dosimetric statistical analysis was performed from dose area product (DAP) and entrance skin dose measured by thermo-luminescent dosimeters localized in the cervical, thoracic and sacral areas. Assessment of the diagnostic quality (phantom and clinical) was realized by independent evaluation by 3 observers, using statistical analysis of quality score and inter-observer reproducibility.

Abbreviations: DAP, dose area product; SSS, slot-scanning system; DFD, dynamic flat-panel detector; AEC, automatic exposure control; CDRAD, contrast-detail radiography phantom; PMMA, polymethyl methacrylate; De, entrance skin dose; TLD, thermo-luminescent dosimeter; IQF, image quality factor; IQFinv, inverse image quality factor; ICC, intraclass correlation coefficient; CI, confidence interval; SD, standard deviation; DQE, detective quantum efficiency.

* Corresponding author. Service d'imagerie anté-natale, de l'enfant et de la femme, Hôpital Pellegrin, place Amélie-Raba-Léon, 33076 Bordeaux cedex, France.
E-mail address: jean-francois.chateil@chu-bordeaux.fr (J.-F. Chateil).

http://dx.doi.org/10.1016/j.diii.2015.06.018

Results: DAP was equivalent with the 2 systems. Entrance skin dose was significantly higher with DFD in thoracic and pelvic regions ($P < 0.05$). Image quality scores of the SSS were significantly better than DFD for a majority of criteria, in both phantom and clinical evaluations.
Conclusion: For scoliosis evaluation, the SSS, compared to the DFD system, offers enhanced image quality while reducing the entrance skin dose in the most radiosensitive areas.

Scoliosis in children and adolescents is a common condition requiring regular radiographic examinations until maturity. Imaging is needed to characterize the type of curve and its severity by evaluating the Cobb angle and spinal axial rotation, but also to identify possible underlying pathologies, to detect any increase in deformation and thus, to help in the decision regarding treatment. Radiographs are the basis of patient evaluation during the initial diagnosis and follow-up, which exposes patients to repeated radiation: reduction of dose is mandatory in daily practice.

Scoliosis examination requires an upright radiograph of the entire spine. Therefore, the most radiosensitive organs such as thyroid gland, mammary glands or gonads are exposed during repeated radiographic examinations, resulting in high-cumulated effective doses [1]. The risks of radiation-induced side effects have been widely discussed in the literature in recent years, especially the possible induction of cancer in children [2,3]. New radiographic systems have become available with the promise of improving radiography while optimizing radiation doses. The appreciation of the dose area product (DAP) is the dosimetric index primarily used in daily practice.

The purpose of this study was to evaluate the radiation dose level and image quality during scoliosis examinations with two digital dynamic systems. These two systems are the slot-scanning system (SSS) (EOS Imaging®, Paris, France) and the dynamic flat-panel detector (DFD) Multidiagnost® Eleva (Philips Medical Systems®, Best, the Netherlands). Two studies were therefore conducted to investigate this issue. The first was a phantom study, with a qualitative and quantitative evaluation of image quality at equivalent dose with the two devices. The second study compared in patients the anatomic quality upon 20 landmarks and the DAP versus regional entrance skin dose by using the two devices.

Materials and methods

Digital radiographic systems

The two devices have undergone regular technique quality checks, thus ensuring their reliability and reproducibility of their properties.

Slot-scanning system

The EOS system is a slot-scanning radiological device that allows simultaneous acquisition of frontal and optional lateral views, especially dedicated to the exploration of osteoarticular disorders, and particularly spinal deformities. The acquisition system, described in previous articles [4—6], is composed of two orthogonal independent couples of tubes and detectors moving vertically at constant speed, scanning the exploration area. The X-ray production system is characterized by a source slot collimation. Base filtration of the X-rays tube is 2.5 mm aluminium with an additional filtration of 1 mm aluminium for the exploration of a whole-spine. The thin beam is strictly perpendicular to the studied object while the whole system is vertically translated. The SSS is a digital radiological device based on a thin gap chamber operating in avalanche mode. The scanning speed in our study was adjusted at 7.6 cm/s. The effective spatial resolution (pixel size) is 193 by 179 μm for a frontal view. The radiographic data collected are stored in digital form for post-processing, measurement of Cobb angle, spinal process rotation, vertical alignment and femur height difference on a specific workstation SterEOS (EOS Imaging®).

Dynamic flat-panel

The Multidiagnost® Eleva is a multifunctional digital radiographic system. The device is remote-controlled and acquisition is possible in the standing and supine positions, the arm moving at constant speed along the child. Base filtration of the X-rays tube is 2 mm aluminium. For exploration of a whole-spine, an additional filtration of 0.1 mm copper and 1 mm aluminium is used, as recommended by the manufacturer. The system is equipped with an automatic exposure control device (AEC), but non-automated exposures are also possible.

The Multidiagnost® Eleva unit uses a digital flat-panel detector Pixium 4700 (Trixell® — Thales Electron Devices, Vélizy, France), 30 × 40 cm. The system performs an acquisition as segmental images at a rate of 3.8 frames per second at the desired height of the exploration for a whole-spine pediatric acquisition. The spatial resolution is 154 μm. The X-ray tube moves longitudinally 2 cm between two successive images. Consecutive images are fused to obtain an overview of the entire spine. This process is called ''stitching'', and is performed with a View Forum Workstation (Philips Healthcare®) running with dedicated software (EasyVision, Philips Medical Systems®). Measurements are performed on the overview image with the same software.

Phantom study

The first part of our study compared the image quality of the two digital systems using a phantom. Observers' perception was evaluated with a contrast-detail radiography phantom (CDRAD 2.0, Artinis Medical Systems®, the Netherlands), to quantify both spatial and contrast resolution, providing a qualitative image quality assessment.

Acquisition modalities

Image quality was assessed with respectively a 5 cm- or 15 cm-thick block of polymethyl methacrylate (PMMA) superimposed on the phantom to simulate the scattering conditions of cervical and lumbar regions. We focused the physics comparison using as reference exam a whole-spine study of a 12-year-old child in order to ensure consistency with the image quality study performed on clinical images. The technical parameters of each device were based on the manufacturers' recommendations for clinical practice: for the SSS, in standard mode as set up in our institution, and for DFD in ''step & repeat with overlap'' mode with AEC. The principle was to apply the reference optimized settings for one system to another, to achieve in ''mirror'' fashion the same acquisitions with the same doses. The air Kerma and the Entrance skin Dose (De) were systematically evaluated by an external ionization chamber controlled by a pair of lithium fluoride thermo-luminescent dosimeters (TLD) (extRad, Kapton®). The DAP was also recorded. This allowed a comparison of image quality under strict dose control. Reference examination conditions (Table 1) were determined as follows:

- for SSS: 85 kV/200 mA/Scanning Speed 7.6 cm/s/air Kerma for 5 cm PMMA and 15 cm PMMA;
- for DFD:
  - cervical spine: 77 kV/500 mA/2 ms/air Kerma for 5 cm PMMA,
  - lumbar spine: 77 kV/500 mA/8 ms/air Kerma for 15 cm PMMA.

CDRAD acquisitions were therefore made on both systems under the same conditions of dose (air Kerma at phantom entrance) and voltage (kV): after setting up the acquisition on the first system with the reference techniques and measuring air Kerma at the phantom entrance, the technique was adjusted in the second system to achieve similar air Kerma (difference < 8%). Four successive experiments, with 2 thicknesses of PMMA each time, were therefore performed (experiments 1 to 4, Table 1). For each acquisition, a single image was obtained with the SSS. For DFD in ''step and repeat with AEC'' mode, four successive overlapped images covering the region of interest were obtained. Therefore, each individual sub-image with DFD received a quarter of the air Kerma (K air DFD 5 cm or K air DFD 15 cm). Reading and scoring of quality was performed on sub-images, and not on the stitched resulting image, as recommended by the manufacturer for clinical practice.

Experimental image quality with phantom

The CDRAD 2.0 phantom consists of a 265 × 265 mm Plexiglas tablet with drilled holes of different depth and diameter (Fig. 1) [7,8]. The image shows 225 squares, left on 15 rows and 15 columns. In each square except in the top three rows, there was one hole in the middle and a second hole randomly located in one of the 4 corners. In each column, the diameter of the holes varied logarithmically from 8 to 0.3 mm, and in each row the depth varied logarithmically from 8 to 0.3 mm. The observer had to indicate in which corner the randomly hole was located. Due to the increasing depth of the holes horizontally, the image shows 15 columns of spots with increasing contrast. The lower detected depth corresponds to the contrast resolution of the image. In the vertical direction, the diameter of the holes increases stepwise, i.e. 15 rows of spots with increasing diameter, which corresponds to the spatial resolution of the image. The best system produces an image in which smaller details and better contrast are visible.

Three observers (one junior radiologist (MH): six years of experience/two seniors radiologists (PB, JFC): over twenty years of experience) read independently all images obtained using the same protocol (3 observers × 2 images × 4 scenarios). Image reading was performed on a dedicated workstation (DXMM DICOM 6.1 SP5, Médasys®, France). This workstation with two 2-megapixel LCD monitors (Radiforce

Table 1 Evaluation of image quality on CDRAD-phantom 2.0.

		kV	mA	Kair (μGy)	De (μGy)	IQFinv				
						Obs 1	Obs 2	Obs 3	Mean	SD
Exp 1	SS System KSS									
	5 cm	85	200	125	165	3.07	3.88	3.33	3.43	0.4
	15 cm	85	200	137	170	1.27	1.81	1.56	1.55	0.3
Exp 2	DFD KSS									
	5 cm	85	500	126	180	2.37	3.55	2.77	2.9	0.6
	15 cm	85	500	126	165	0.88	1.04	1.05	0.99	0.1
Exp 3	SSSystem KDFD									
	5 cm	77	125	97	125	2.47	3.51	2.93	2.97	0.5
	15 cm	77	500	504	690	2.14	2.78	2.47	2.46	0.3
Exp 4	DFD KDFD									
	5 cm	77	500	95	135	2.06	2.68	2.8	2.51	0.4
	15 cm	77	500	494	690	1.54	1.92	2.08	1.85	0.3

On rows: four successive experiments. Experiments 1 and 2: acquisition at SS system optimized air Kerma (KSS) with SS system (exp 1) and DFD (exp 2). Experiments 3 and 4: acquisition at DFD optimized air Kerma (KDFD), with SS System (exp 3) and DFD (exp 4). On columns: exposure values (kV: kilovolts, mAs: milliAmper per second), Kair: air Kerma in μGray, De: entrance skin dose in μGray, and IQFinv: inverse Image Quality Factor for each experience and observer.

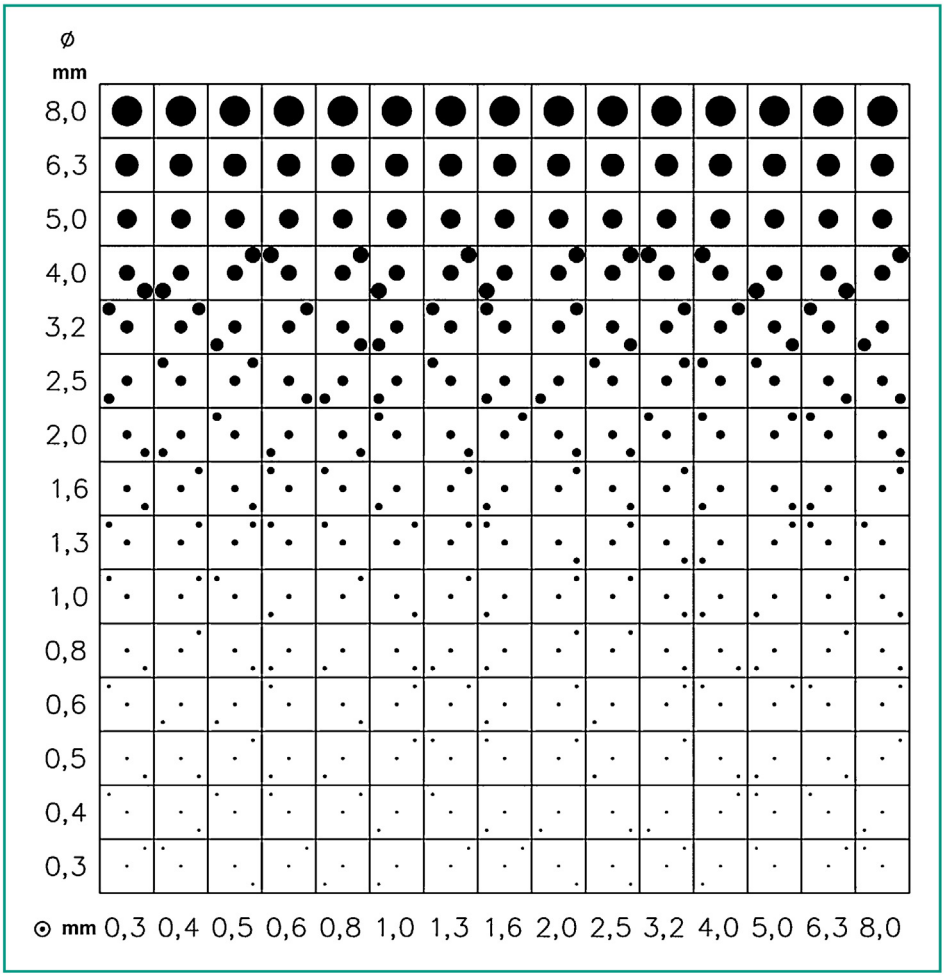

Figure 1. Schematic representation of the CDRAD-phantom: within a row the hole-diameter is constant, with exponentially increasing depth, and within a column the hole-depth is constant, with exponentially increasing diameter [8].

RS 210, 21.3″, Eizo®, Japan) had previously been calibrated specifically for reading this type of examination, and allowed a varying dynamic contrast grayscale on 10^5-bit with a 1200×1600 pixels resolution for each screen.

Data analysis for phantom study

Data analysis was based on the CDRAD methodology suggested by Thijssen et al. [8]. From these data, a numerical value, the Image Quality Factor (IQF), is calculated. The IQF is defined as the sum of the products of depth and diameter for correctly limiting the identified randomly corners' holes in the phantom. To highlight the differences between the two radiologic systems, we used the ''IQFinv'' meaning Inverse Image Quality Factor (IQFinv = 1/IQF). A higher IQFinv indicates better image quality. An IQFinv was assigned to each CDRAD image (average for the three observers). Statistical analysis of performance of the three observers was computed (XLStat®, Addinsoft®, France). Descriptive data were reported as charts, percentages, means and standard deviations (SD). The normality of the continuous variables was assessed prior to the application of parametric methods. Student's test was used to compare the ''IQFinv'' obtained for the two methods by each observer. Inter-observer reproducibility was evaluated by intraclass correlation. Statistical significance was defined as a *P*-value less than 0.05.

Qualitative clinical study and dose evaluation

Patients

Sixty-one children and adolescents who underwent a scoliosis examination were included prospectively. The local research ethics committee (Committee for Protection of Persons Participating in Biomedical Research) approved the study and validated its strictly observational character. Informed consent was obtained from the parents or relatives of each child. All imaging studies were performed as routine examinations. The patients were alternatively directed to each modality when making appointments provided by the secretarial staff, unbeknown to the investigators of the study. For each child, age, sex, height and weight were systematically recorded. Body mass index was calculated and plotted on standardized curves according to age.

Technique of acquisition

Examination procedure

Standing whole-spine frontal radiographs were taken on the SSS or DFD. The acquisition was systematically done with a postero-anterior beam. The field of acquisition concerned the region from the base of the skull to the tip of the coccyx and extended from one iliac crest to the next.

With SSS, the distance between the X-ray source and the detector was 130 cm. The child was positioned 96 cm from the source according to a predefined isocentric benchmark. At our institution, the width of the image field remained constant (39 cm), according to the manufacturer's recommendations.

With DFD, the distance between the X-ray source and the detector was 125 cm. The radiation field could be collimated in width by using a light beam, to be adapted to the morphology of each subject.

For each examination, the exposure factors selected by the radiographer were recorded: tube voltage (kV), intensity (mAs), focal distance between tube and patient, and size of the radiation field at the surface of the child, both being measured with a tapeline, to calculate the entrance exposed area.

Evaluation of image quality in clinical study

Images were read independently under identical conditions by the same 3 radiologists. Reading was done with knowledge of the radiological technique used, because of inherent differences in each device: single image with SSS, set of original native and stitched images with DFD. With the latter, anatomic quality was evaluated on native images, and Cobb evaluation on stitched images.

Diagnostic image quality was assessed using a list of 20 anatomical criteria established from the ''European Guidelines on Quality Criteria for Diagnostic Radiographic Images'' [9] and suitable for a thorough analysis of scoliosis [5]. Nineteen were criteria concerning visibility of anatomical structures (vertebral body, pedicles, spinous process at each vertebral level, femoral heads, sacrum, posterior inferior iliac process, clavicles, chest, mediastinal lines, and degree of ossification of the iliac crest, defined as Risser Index). Each criterion was rated from 0 to 3, according to the less visible structure for each criterion: 0: structure not detectable; 1: Structure visible but features not perceptible; 2: features discernible but not clearly defined; 3: features clearly defined. The 20th criterion was the possibility for the observer to determine reliably and accurately the Cobb angles. An independent measurement (one or two curvatures) was performed by each observer for each image according to pre-established levels benchmarks provided to the reader. Observers benefited from a training phase performed beforehand on a set of images not included in the study cohort.

Dose evaluation in clinical study

The radiation dose was evaluated in two ways.

Dose area product

The DAP, expressed in $cGy.cm^2$, was automatically given by both radiographic systems. DAP was calculated by each system software from a polynomial approximation based on physical acquisition parameters and validated by the manufacturers.

Entrance skin dose: De

For each child, three pairs of Lithium Fluoride TLD provided by the Institute for Radiological Protection and Nuclear Safety (IRSN, Fontenay-aux-Roses, France) were exposed. They were placed on the back, next to the most radiosensitive organs to estimate the locally delivered irradiation: cervical (thyroid), interscapular (mammary) and sacral (genitals) regions. The TLD were attached with paper plaster to the skin at the point of intersection with the central axis beam, closed to the midline. After being exposed to ionizing radiation, reading of dosimeters was conducted by the IRSN using an automatic reader Harshaw TLD 8800 (Thermo Fisher Scientific Inc®, Germany) and each value was recorded. Control non-exposed TLD, always kept outside the examination room, were used to remove background for each set of TLD. The averaged De was evaluated for each pair of dosimeters for the three regions of interest.

Statistical analyses for clinical study

To prevent double-dose irradiation, children were either assigned to the SSS group or to the DFD group. The normality of the continuous variables of this population was assessed prior to the application of parametric methods to compare the two-irradiation skills for dose delivery. To evaluate the quality of radiographic images, statistical significance using the Chi^2 test was defined as a *P*-value less than 0.05 between the two radiographic systems for each criterion. Total score (sum of each criterion) was evaluated with Student's test for each observer. Inter-observer reproducibility between the three evaluators was tested globally for the 20 items and for Cobb angle and Risser index specifically. Reproducibility was estimated using the intraclass correlation coefficient (ICC) and its 95% confidence interval (CI) in a mixed linear regression model after verifying normality and homoscedasticity. Statistical analyses were performed using SAS® software version 9.1.3 (SAS Institute Inc, United States).

Results

Image quality on phantom

For each observer taken individually, IQFinv of the SSS was better than DFD (observer 1 $P = 0.006$, observer 2 $P = 0.011$, observer 3 $P = 0.025$). The average IQFinv for the 3 observers was significantly better for the SSS. Regardless of the experiment under review, the SSS outperformed the DFD on image quality ($P < 0.001$). The results for each experiment are also represented on graphs: the contrast resolution curves (lines connecting the central spots with the smallest visible diameter and contrast for each modality) were established from IQFinv means for each experiment.

Fig. 2 shows the mean for the 3 readers of the IQFinv values and the mean contrast resolution curves obtained on the two systems for 5 and 15 cm PMMA with SSS reference dose conditions. Curves close to the axes means better image quality. Visualizing the contrast-detail curve closer to the lower left corner of the graph corresponds to visualization of smaller and/or lower contrast-details. The

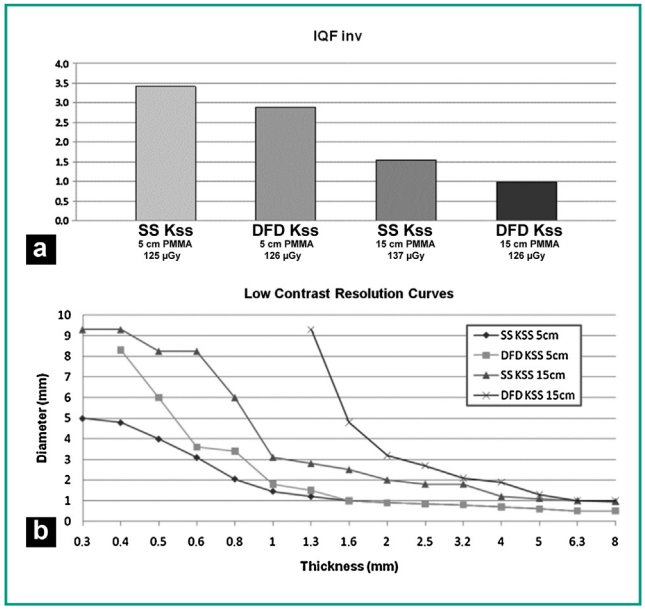

Figure 2. Evaluation of image quality on CDRAD-phantom 2.0 with optimized SSS parameters: a: mean calculated IQFinv values obtained under dose control with optimized SSS parameters (KSS) with 5 cm and 15 cm PMMA applied to SSS and DFD; air Kerma for each experiment; b: contrast-detail curves obtained with SSS parameters with 5 cm and 15 cm PMMA applied to SSS and DFD.

SSS outperformed the DFD in both small and large absorption areas. It was also significantly better for contrast resolution ($P < 0.05$).

Fig. 3 shows the mean of the IQFinv values and the mean contrast resolution curves obtained on the two systems for 5 and 15 cm PMMA with DFD reference dose conditions.

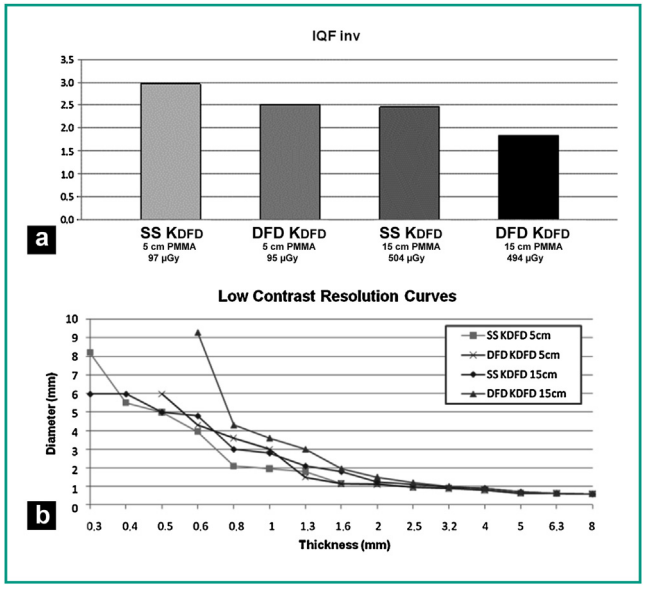

Figure 3. Evaluation of quality image on CDRAD-phantom 2.0 with optimized DFD parameters: a: mean calculated IQFinv values obtained under dose control with optimized DFD parameters (KDFD) with 5 cm and 15 cm PMMA applied to SSS and DFD; air Kerma for each experiment; b: contrast-detail curves obtained with DFD parameters with 5 cm and 15 cm PMMA applied to SSS and DFD.

Table 2 Image quality with CDRAD-phantom inter-observer reproducibility by intraclass correlation measurement.

	SS System	DFD
Single measurement	0.98	0.90
95% confidence interval	0.87—0.99	0.52—0.99
Average measures	0.99	0.96
95% confidence interval	0.95—1	0.77—0.99

Despite parameters optimized for DFD acquisitions, the SSS again outperformed the DFD at equivalent dose in both small and large absorption areas, and gave significantly better contrast resolution ($P < 0.05$).

The inter-observer reproducibility evaluated by intraclass correlation measurement from the four experiments is given in Table 2. Results show less variability between readers on SSS images, with higher values within 95% confidence interval.

Clinical results

Assessment of study population

The study population consisted of 61 children (44 females and 17 males). Thirty-two were examined on the SSS and 29 on the DFD. Four children considered overweight (body mass index above the 97th percentile for age) were excluded in order to harmonize the two groups: one in the SSS group, and 3 in the DFD group. Finally, a cohort of 57 children was selected: thirty-one (22 females, 9 males) were examined with the SSS and 26 (18 females, 8 males) with the DFD.

The population distribution is shown in Table 3. The mean age was 11.4 years (SD = 2.64) in the SSS group and 11.3 (SD = 1.87) in the DFD group. The distribution of age and body mass index was similar in both groups, as was gender distribution with 70% of girls and 30% of boys. There was no

Table 3 Comparison of the two populations.

	SS System	DFD	Total
Population			
n	31	26	57
Age (years)			
Average	11.45	11.35	
SD	2.64	1.87	
Median	12	11.5	
Gender			
Females	22 (71%)	18 (69%)	40 (70%)
Males	9 (29%)	8 (31%)	17 (30%)
BMI (kg.m^2)			
Average	16.4	16.79	
SD	2.2	2.27	
Median	16	16,3	

There was no difference in age, gender, and body mass index (BMI) distribution between the two groups of patients ($P = 0.87$).

Table 4 Image quality evaluation.

Anatomical criteria	Comparison between SS system and DFD[a]
Cervico-dorsal spine	
Vertebral bodies	SS System > DFD[b]
Pedicles	SS System > DFD[b]
Transverse processes	SS System > DFD
Spinous process	SS System > DFD
Dorsal spine	
Vertebral bodies	SS System > DFD
Pedicles	SS System > DFD
Transverse processes	SS System > DFD
Spinous process	SS System > DFD
Lumbar spine	
Vertebral bodies	SS System > DFD
Pedicles	SS System < DFD[b]
Transverse processes	SS System < DFD[b]
Spinous process	SS System < DFD[b]
Pelvis	
Femoral heads	SS System < DFD[b]
PIIS	SS System > DFD
Sacrum	SS System < DFD[b]
Risser index estimation	SS System > DFD[b]
Others	
Clavicles	SS System > DFD
Chest	SS System > DFD[b]
Mediastinal lines	SS System > DFD
Cobb angle evaluation	SS System > DFD

Score for the 20 anatomical criteria were calculated for the 3 observers.
[a] Mean values of results for each criterion obtained by the 3 observers, Chi^2 square test.
[b] $P \leq 0.05$. SS System: slot-scanning system; DFD: dynamic flat detector.

difference in population distribution per type of device used ($P = 0.87$).

Clinical image quality results

Table 4 shows the evaluation made by the three observers on 20 appropriate criteria concerning the anatomical analysis. Overall, results were better with the SSS with regard to the cumulative score, but only significant for one observer (observer 1 $P = 0.03$, observer 2 $P = 0.46$, observer 3 $P = 0.05$). The difference was not significant on most criteria, even though the SSS tended to perform better on part of them: the SSS was significantly superior for visualizing the cervical spine, the thoracic cage, and the ability to determine the Risser index. The DFD system was significantly superior for visualizing the lumbar spine, femoral heads and sacrum. Inter-observer reproducibility for the global score (20 items) between the three evaluators was better for the SSS (ICC = 0.58, 95%CI: 0.29—0.77) relative to DFD (ICC = 0.35, 95%CI: —0.2—0.63). For the Cobb angle measurement, ICC was 0.98 (95%CI: 0.95—0.99) for the SSS and 0.96 (95%CI: 0.91—0.99) for the DFD.

Table 5 Dose area product (DAP) in $cGy.cm^2$ directly calculated by the two radiographic systems.

	SS System	DFD
DAP ($cGy.cm^2$)		
n	31	26
Average	39.8	41.3
SD	11.7	20.6
Median	42.2	40.2

Median test: $P = 0.68$.

Clinical dosimetry results

The average and median values of the DAP are given in Table 5. There was no significant difference observed between the 2 groups ($P = 0.68$). Entrance skin doses recorded with the TLD are given in Table 6. The median dose observed with the SSS was 1.57 times significantly higher than with the DFD ($P < 0.001$) for the cervical region, and was 1.49 and 2.15 times significantly lower than with the DFD for the thoracic and sacral regions, respectively ($P < 0.001$).

Discussion

Plain X-rays of the whole-spine in children and adolescents are responsible for relatively higher doses than in other conventional procedures. Total radiation risk is best quantified by the use of the effective dose, which is a reliable measure of the stochastic risk for the induction of cancer. The mean effective dose observed with one postero-anterior whole-spine exposition, which covers a large part of the body and may be responsible for high cumulative doses, ranges from 0.05 to 0.5 mSv [10,11]. Supplementary lateral views and follow-up studies (up to 20 during adolescence) increase the cumulative effect and may be responsible for a significant dose delivered to the thyroid, breast and genitals. The organ effective dose takes into account the doses received by all radiosensitive organs and weighted by the radiosensitivity of each one of them. Organ weighting factors are currently specified by the International Commission on Radiological Protection: gonads: 0.08, breast: 0.12, thyroid 0.04 [12]. The main risk seems to be the exposure of the mammary gland during puberty. The mean estimated cumulative dose to the breast ranges from 0.3 to 10.9 cGy [13,14], leading to a relative risk of breast cancer mortality that was found to be significantly increased in previous studies, using systems not allowing dose reduction. The potential risk of multiple radiographic examinations especially in the management of scoliosis, has led to efforts to reduce patient exposure on the basis of the ALARA principles [1,3,12,15]. This includes using postero-anterior instead of antero-posterior exposure to limit mammary exposure, limiting the number of radiographs (only frontal view in the follow-up), and development of competing digital technologies.

The DAP provided by our digital devices is calculated by the software within the computer of the device and is

Table 6 Entrance skin dose (De in μGy) measured for each radiographic system by thermo-luminescent dosimeters on the three regions of interest.

	Cervical De (μGy)		Dorsal De (mGy)		Sacral De (μGy)	
Radiographic System	SS System ($n = 31$)	DFD ($n = 26$)	SS System ($n = 31$)	DFD ($n = 26$)	SS System ($n = 31$)	DFD ($n = 26$)
Average	172.8	122.9	181.5	316.3	189	524.6
SD	45.3	41.2	48.3	143	48.8	247.3
Min	63	55	54	16	54	209
Median	183	116.5	195	290.5	202	435.5
Max	248	265	248	874	270	1117
Median Test	$P < 0.001$		$P < 0.001$		$P < 0.001$	

obtained by a polynomial approximation based on physical acquisition parameters validated by the manufacturers. In our series, exposure data were obtained with a different mode for each technique: line-by-line for the SSS, successive exposures with a partially superimposed rectangular field of view for DFD. The DAP estimation algorithm in both systems takes into account the following factors in calculating an estimate: kVp, mAs, mGy/mAs (overall tube output), source-to-detector distance, field of view, scanning speed (SSS), collimator spectral filtration and presence of antiscatter grid (DFD).

In our study, we did not find any significant DAP difference between the two techniques. We also included the role of the total exposed surface in calculating the DAP. While the total height was comparable in our two populations, the lateral collimation was slightly different, and the surface area was somewhat larger with the SSS in terms of ''total irradiated area''. On the other hand, more than 20 elementary surfaces were superimposed with the DFD, because stitching process needs an overlapping for a better result; the total area exposed was therefore greater.

The two systems have significant technical differences as outlined above, so their methods for calculating the DAP are necessarily different. The first conclusion is that the DAP may lack accuracy when calculating the dose delivered in such cases. Even so, DAP remains widely used because it is the simplest way to assess the dose, even approximately, and to be sure that the threshold is not being exceeded, when diagnostic reference levels are available.

The entrance skin dose is the conventional method used for assessing the dose delivered to a given anatomical region. A sensor recording the cumulative dose of the incident radiation and radiation scattered by the patient is useful to measures it. In our study, the dose varied for the successive anatomical regions with DFD, whereas it was constant for the SSS; this was due to the acquisition mode: exposure parameters remained constant throughout the scan with the SSS, while the AEC control changed the intensity for each exposure with the DFD, in relation to the observed absorption. The observed dose was lower in the cervical region with the DFD, whereas it was significantly higher at the thoracic level (×2) and sacral level (×3) with the DFD. Thus the delivered dose to each anatomical region and subsequent organs was different. For example, it was lower for the cervical spine and thyroid with the DFD, and lower for the breast and genitals with the SSS. Difference in delivered doses with the two devices is still lower than the one observed in other studies [16].

Assessment of the dose to each organ requires a Monte Carlo calculation, as described in NRPB [17], or experimental measures with anthropometric phantoms [18]. We did not perform such simulation in our study. Other studies have shown that with a mean entrance dose of 181 and 316 μGy with SSS and DFD respectively, effective doses range from 0.08 to 0.20 mSv [5,19—23]. Given the skin entrance dose observed in our study, the dose ratio is better for the SSS. Table 7 shows skin entrance doses and other dosimetric values observed in previous studies. The exposition values observed with our two devices are within the lower values of the range of doses.

Detective quantum efficiency (DQE) is a measure of the combined effect of noise and contrast performance [24]; it is widely recognized as an accurate evaluation of detector performances that combines in a single measurement the usual detector characteristics of spatial resolution (the Modulation Transfer Function) and noise behaviour over the useful spatial frequency spectrum. The DQE standard from IEC mentions specifically that DQE is not suited and should not be evaluated for systems in which the X-ray field is scanned across the patient [25]. Evaluating SSS, Damet et al. found a DQE peak around 13% (RQA5 and RQA7), but confirmed that DQE for SSS must not be directly compared to DQE values for 2D radiography systems [23]. Therefore, in our study we evaluated the quality of the two systems with another parameter, i.e. the IQFinv using a CDRAD-phantom with the clinical reference parameters of each device. The SSS clearly showed the better IQFinv with each set of parameters, and the difference was significant. Even with the reference parameters adjusted for each device corresponding to the higher dose for the CPD, sensitivity in contrast and resolution was better with the SSS, mainly with the thicker PMMA interposition simulating the sacral anatomic region. Nevertheless comparing the image quality of both devices in phantom study is limited by the fact that we used both devices in their usual configuration. This implies that the hardness of the X-ray beam was not exactly similar, because filtration of radiation beam is obviously specific to each system. For our study on CDRAD-phantom, we used an identical voltage of 85 kV for SSS and DFD, but the entrance exposures are really comparable if two systems have the same beam quality: same voltage and identical half-value layer attenuation.

Table 7 Comparison with the recent literature data: dosimetric values observed in our study and previous studies [5,19—22].

Study	Radiographic system	Dose measure-ment	Examination	Age (years)	KVp Mean	mA Mean	mAs Mean	De Cervical µGy	De Dorsal µGy	De Sacral µGy	Average De µGy	DAP cGy.cm^2	KAP cGy.cm^2	Effective Dose mSv
Our study 2011 (median values)	SS System (EOS Imaging®)	TLD	Whole-Spine PA	11.45 SD 2.64	85	190	0.63	183	195	202		42.21 SD 11.71		
	DFD (Eleva Multidiag-nost Philips®)		Whole-Spine PA	11.35 SD 2.87	78	500	NA	116.5	290.5	435.5		40.25 SD 20.65		
	Ratio DR/SS System							0.64	1.49	2.15		1.04		
Deschenes et al., 2010 [5]	SS System (EOS Imaging®)	OSLD	Whole-Spine PA and LAT	14.8 SD 3.6	NS	NS		200	180	300				
	CR (FCR 7501S Fuji®)		Whole-Spine PA and LAT	14.8 SD 3.6	NS	NS		590	1040	2470				
	Ratio CR/SS System							2.9	5.9	8.2				
Grieser et al., 2010 [19]	DFD (Digital Diagnost Philips®)		Whole-Spine AP	16 SD 5.7	80	NS						168		
Dubousset et al., 2005 [20]	SS System (EOS Imaging®)		Whole-Spine PA								127			
	Screen Film imaging		Whole-Spine PA								1196			
	Ratio										9.4			
Gogos et al., 2003 [21]	Screen Film imaging	TLD	Whole-Spine AP	8—12	76	8.1					819			
				13—18	78.5	9.3					1074			

Table 7 (*Continued*)

Study	Radiographic system	Dose measure-ment	Examination	Age (years)	KVp Mean	mA Mean	mAs Mean	De Cervical μGy	De Dorsal μGy	De Sacral μGy	Average De μGy	DAP cGy. cm^2	KAP cGy. cm^2	Effective Dose mSv
Geijer et al., 2001 [22]	DR (Multi Diagnost 4 Philips®)	TLD	Whole-Spine PA		70	NS					900		87	0.15
	Digital Fluoroscopy (Multi Diagnost 4 Philips®)				64	NS					510		9.7	0.015
	Screen Film imaging				66	40					110		43	0.086

AP/PA: antero-posterior/postero-anterior; DR: digital radiography; De: entrance skin dose; KAP: Kerma area product; OSLD: optically stimulated luminescent dosimeters; SD: standard deviation.

Due to technical particularities and properties of each device, such as filtration (3.5 mm aluminium with SSS; 3 mm aluminium + 0.1 mm copper for DFD for whole-spine acquisition, as recommended by the manufacturers), involving slightly different half-value layer attenuation, the hardness of the X-ray beam is not strictly identical for both devices. This observation limits the equivalence of doses even if we took care to use the same voltage and to control the air Kerma, during the CDRAD-phantom acquisitions. Nevertheless we used both systems in their commercial configuration and their clinical settings, prior to the clinical study.

Technical simulations such the one we performed on phantoms are required to determine optimal operating conditions, to reproduce the physics of the detection process and to explore the effect of different acquisition parameters on the resulting image. Nevertheless, the ultimate objective of these technical improvements is to obtain a sufficient image quality to establish a diagnosis. An evaluation of the two devices in a clinical situation was therefore essential for correlation with the subjective quality of images as perceived by a human observer. One limitation of our study is that children only underwent one of the 2 examinations, to avoid a double exposition; we tried to avoid any bias by comparing our two populations, and demonstrated any significant difference. Results were better with the SSS with regard to the cumulative score, cervical and dorsal spine. On the cervical area, this could be due to the relatively higher dose delivered with the SSS compared to the DFD. Reproducibility of the Cobb angle was also better with the SSS, with a lower dispersion of results: this good reproducibility with SSS was also founded by other studies [26]. The better IQFinv observed with the phantom study was not transposed into a measurable significant advantage in the clinical study when applied to the lumbar spine. This lack of significant difference observed may be due to the fact that the latter is a bony structure with a natural high contrast level and low frequency details.

The SSS provides a higher image quality-to-dose ratio for scoliosis imaging using the combined advantages of dose-efficient detection. Advanced post-processing also allows 3D simulation of bony structures obtained by simultaneous acquisition of two orthogonal radiographic views [4,6]; SSS can also be used for other applications, such lower limbs evaluation or pelvimetry in pregnant women [27]. The anatomical areas best explored by the SSS are mainly the spine, pelvis and lower limbs. However, one of the advantages but also a limitation of the SSS is the need to perform examinations only in a standing position, which could limit its use in clinical practice (i.e. appreciation of reducibility of spinal curvature in decubitus position). Regarding the assessment of scoliosis, exposure with lateral bending can be performed with SSS [6] but there is a need to compare with conventional studies performed in decubitus position, with less muscle contraction. Scoliosis in patients suffering neuromuscular diseases could also be difficult to analyse with SSS, as they cannot stand alone, which is rather not their usual functional position.

On the other side, the dynamic properties, larger field of view and possibility of software stitching provided by the DFD has broadened the range of clinical applications that can be supported by flat-panel detectors (i.e. whole-spine radiography in supine position, which is useful for assessing the reducibility of a spinal curve, or in neuromuscular diseases, with non-standing patients). Multiple other radiographic studies could also be performed with this device. DFD system still represents an alternative if a more polyvalent device is required for units with varied activities.

Conclusion

A whole-spine examination may be performed today in several ways, so it is useful to know how the patient dose varies with the X-ray device used. Our data demonstrate the relative inaccuracy of the DAP in terms of precise dosimetry for a whole-spine study, but the DAP remains primarily a practical dosimetric indicator, allowing the physician to appreciate the dose level used compared to the guidelines or diagnostic reference levels, when available. The present prospective study investigated the value of two recent devices for the diagnosis of adolescent scoliosis. Results indicate significant dose savings with an equivalent or superior image quality with both devices. These exposure reductions were obtained without significant loss in image quality and in most instances with an improvement in the overall quality due to the more uniform exposure. SSS should be the best settlement regarding dose and image quality for spine and lower limbs examinations.

Author contributions

Guarantors of integrity of entire study, M.Y., JF.C.; study concepts/study design or data acquisition or data interpretation, M.Y., JF.C., P.B., JL.R.; manuscript drafting or manuscript revision for important intellectual content, all authors; manuscript final version approval, all authors; literature research, M.Y., JF.C.; experimental studies, M.Y., JF.C., JL.R.; statistical analysis, A.D., E.L., M.Y., JF.C.; and manuscript editing, all authors.

Disclosure of interest

The authors declare that they have no conflicts of interest concerning this article.

References

[1] Nash Jr CL, Gregg EC, Brown RH, Pillai K. Risks of exposure to X-rays in patients undergoing long-term treatment for scoliosis. J Bone Joint Surg Am 1979;61:371—4.
[2] Doody MM, Lonstein JE, Stovall M, Hacker DG, Luckyanov N, Land CE. Breast cancer mortality after diagnostic radiography: findings from the U.S. Scoliosis Cohort Study. Spine (Phila Pa 1976) 2000;25:2052—63.
[3] Bone CM, Hsieh GH. The risk of carcinogenesis from radiographs to pediatric orthopaedic patients. J Pediatr Orthop 2000;20:251—4.
[4] Despres P, Beaudoin G, Gravel P, de Guise JA. Physical characteristics of a low-dose gas microstrip detector for orthopedic X-ray imaging. Med Phys 2005;32:1193—204.
[5] Deschenes S, Charron G, Beaudoin G, Labelle H, Dubois J, Miron MC, et al. Diagnostic imaging of spinal deformities: reducing patients radiation dose with a new slot-scanning X-ray imager. Spine (Phila Pa 1976) 2010;35:989—94.

[6] Ilharreborde B, Dubousset J, Le Huec JC. Use of EOS imaging for the assessment of scoliosis deformities: application to postoperative 3D quantitative analysis of the trunk. Eur Spine J 2014;23(Suppl 4):S397—405.
[7] Thijssen MA, Thijssen HO, Merx JL, van Woensel MP. Quality analysis of DSA equipment. Neuroradiology 1988;30: 561—8.
[8] Thijssen M, Bijkerk H, van der Burght R. Manual CDRAD-phantom type 2.0. Project quality assurance in radiology. St. Radboud, The Netherlands: Department of Radiology; 1998.
[9] European Commission. European guidelines on quality criteria for diagnostic radiographic images in paediatrics. Luxembourg: Office for official publications of the European communities; 1996.
[10] Gialousis G, Yiakoumakis EN, Makri TK, Papadoupoulou D, Karlatira M, Karaiskos P, et al. Comparison of dose from radiological examination for scoliosis in children among two pediatric hospitals by Monte Carlo simulation. Health Phys 2008;94:471—8.
[11] Hansen J, Jurik AG, Fiirgaard B, Egund N. Optimisation of scoliosis examinations in children. Pediatr Radiol 2003;33: 752—65.
[12] ICRP. The 2007 Recommendations of the International Commission on Radiological Protection. ICRP publication 103. Ann ICRP 2007;37:1—332.
[13] Levy AR, Goldberg MS, Mayo NE, Hanley JA, Poitras B. Reducing the lifetime risk of cancer from spinal radiographs among people with adolescent idiopathic scoliosis. Spine (Phila Pa 1976) 1996;21:1540—7.
[14] Ronckers CM, Land CE, Miller JS, Stovall M, Lonstein JE, Doody MM. Cancer mortality among women frequently exposed to radiographic examinations for spinal disorders. Radiat Res 2010;174:83—90.
[15] Doody MM, Freedman DM, Alexander BH, Hauptmann M, Miller JS, Rao RS, et al. Breast cancer incidence in U.S. radiologic technologists. Cancer 2006;106:2707—15.
[16] Wade R, Yang H, McKenna C, Faria R, Gummerson N, Woolacott N. A systematic review of the clinical effectiveness of EOS 2D/3D X-ray imaging system. Eur Spine J 2013;22: 296—304.
[17] Hart D, Hillier MC, Wall BF. National reference doses for common radiographic, fluoroscopic and dental X-ray examinations in the UK. Br J Radiol 2009;82:1—12.
[18] Seidenbusch M, Schneider K. Conversion coefficients for determining organ doses in paediatric spine radiography. Pediatr Radiol 2014;44:434—56.
[19] Grieser T, Baldauf AQ, Ludwig K. Radiation dose reduction in scoliosis patients: low-dose full-spine radiography with digital flat panel detector and image stitching system. Rofo 2011;183:645—9.
[20] Dubousset J, Charpak G, Dorion I, Skalli W, Lavaste F, Deguise J, et al. A new 2D and 3D imaging approach to musculoskeletal physiology and pathology with low-dose radiation and the standing position: the EOS system. Bull Acad Natl Med 2005;189:287—300.
[21] Gogos KA, Yakoumakis EN, Tsalafoutas IA, Makri TK. Radiation dose considerations in common paediatric X-ray examinations. Pediatr Radiol 2003;33:236—40.
[22] Geijer H, Beckman K, Jonsson B, Andersson T, Persliden J. Digital radiography of scoliosis with a scanning method: initial evaluation. Radiology 2001;218:402—10.
[23] Damet J, Fournier P, Monnin P, Sans-Merce M, Ceroni D, Zand T, et al. Occupational and patient exposure as well as image quality for full spine examinations with the EOS imaging system. Med Phys 2014;41:063901.
[24] Cowen AR, Davies AG, Sivananthan MU. The design and imaging characteristics of dynamic, solid-state, flat-panel X-ray image detectors for digital fluoroscopy and fluorography. Clin Radiol 2008;63:1073—85.
[25] IEC. Medical electrical equipment — Characteristics of digital X-ray imaging devices — Part 1: determination of the detective quantum efficiency. Genève: International Electrotechnical Commission; 2003.
[26] Ilharreborde B, Steffen JS, Nectoux E, Vital JM, Mazda K, Skalli W, et al. Angle measurement reproducibility using EOS three-dimensional reconstructions in adolescent idiopathic scoliosis treated by posterior instrumentation. Spine (Phila Pa 1976) 2011;36:E1306—13.
[27] Sigmann MH, Delabrousse E, Riethmuller D, Runge M, Peyron C, Aubry S. An evaluation of the EOS X-ray imaging system in pelvimetry. Diagn Interv Imaging 2014;95:833—8.